Morphology of poly(*p*-phenylene sulfide)/polyethylene blends

T. H. Chen and A. C. Su*

Institute of Materials Science and Engineering, National Sun Yat-Sen University, Kaohsiung, Taiwan 80424, ROC

(Received 16 March 1993)

Blends of poly(*p*-phenylene sulfide) (PPS) and polyethylene (PE) of various component ratios were prepared via melt mixing in a laboratory-scale internal mixer. Cryogenically fractured surfaces of these blends were examined by means of scanning electron microscopy. General morphological features including the domain size and the phase inversion process were discussed in terms of droplet dispersion during melt mixing and phase coarsening after cessation of flow. Interestingly, the surface of dispersed PE particles showed distinct features of protruding fibrils whereas the surface of dispersed PPS particles was characterized by an orange-peel appearance. These were explained in terms of the sequential crystallization of the two phases and the loose packing of PPS crystallites in the intermediate stage of solidification.

(Keywords: blend morphology; poly(*p*-phenylene sulfide); polyethylene)

INTRODUCTION

The properties of blends of immiscible polymers are often closely related to the phase morphology. It is well known that the mechanical properties of rubber-toughened plastics depend strongly on the particle size and volume fraction of the dispersed rubber phase[1,2]. For immiscible blends of intermingled, co-continuous phases, interesting properties (such as increased melt elasticity[3] and more-than-additive modulus in all directions[4]) may arise. More specifically, the retention of thermoplastic processibility and rubber-like resilience may be achieved for thermoplastic/rubber blends with co-continuous phases[5].

As comprehensively reviewed on several occasions[6–8], the particle size in melt-mixed blends of the domain-in-matrix morphology may be affected by material parameters (such as viscosity, elasticity and interfacial tension of the component phases) as well as process parameters (such as the mode and the rate of the mixing action). Under fixed processing conditions, it may be summarized qualitatively that the domain size tends to (a) decrease with the matrix viscosity and the matrix elasticity and (b) increase with the interfacial tension, the disparity in phase viscosity and the volume fraction of the dispersed phase.

Dual-phase continuity can often be realized via mechanical blending of immiscible polymers[3,5,9–13]. It is generally observed that a phase inversion process proceeds gradually with the variation in blend composition; within this composition range of phase inversion, co-continuous phases may appear. On the basis of experimental observations that the phase with lower viscosity (η) or higher volume fraction (ϕ) tends to form the continuous phase in typical two-phase systems[14,15], Sperling *et al.*[10] proposed a simple expression for the prediction of the central composition of the phase inversion region:

$$\phi_1/\phi_2 = \eta_1/\eta_2 \quad (1)$$

in which subscripts 1 and 2 represent the two phases.

We have recently examined the processing–morphology–property relationship of poly(*p*-phenylene sulfide)/polyethylene (PPS/PE) blends. Reported here are observations on the domain-size behaviour, the phase inversion process and some interesting features of the PPS/PE interface in these blends.

EXPERIMENTAL

Materials

Two commercial PPS samples (namely, Ryton® P-4 and V-1 from Phillips Petroleum) were used. The former (hereafter designated as PPSH) was a high-viscosity, extrusion-grade material with a melt flow index (*MFI*, measured at 315°C under a ram load of 5 kg) value of 60 dg min^{-1}. The latter (hereafter designated as PPSL) was a low-viscosity material for powder coating applications; the *MFI* value was ca. 5000 dg min^{-1}. According to the gel permeation chromatographic (g.p.c.) results of Stacy[16], PPSH should be a lightly branched polymer (trichlorobenzene comonomer content = 0.13 mol%) with $M_w \simeq 7.5 \times 10^4$ and PDI ($= M_w/M_n$) $\simeq 1.5$, whereas PPSL is a linear polymer with $M_w \simeq 2.4 \times 10^4$ and $PDI \simeq 1.3$.

The high-density polyethylene sample (hereafter designated as PE), with specific gravity = 0.961, $M_w \simeq 1.4 \times 10^5$, $PDI \simeq 4$ (high-temperature g.p.c., using *o*-dichlorobenzene as the carrier solvent) and $MFI = 6.5$

* To whom correspondence should be addressed

0032-3861/93/234826-06

dg min^{-1} (measured at 190°C under a ram load of 2.16 kg), was obtained from USI Chemical. Estimated[17] values for the specific volumes of PPS and PE at 300°C were 0.83 and 1.38 $cm^3\ g^{-1}$, respectively. These were used in the conversion of blend composition from weight fraction to volume fraction at 300°C.

Melt mixing

Melt blending was performed by use of a Brabender-type mixer (Haake–Buchler Rheomix® 600 connected to the Rheocord® 40 main frame, equipped with a pair of high-shear roller-type rotors). The component polymers were fed under a nitrogen blanket into the preheated mixer and melt mixed at 300°C for 12 min under a fixed rotor rate of 40 rpm. The value of mixing torque near the end of melt mixing was taken to represent the viscosity level[10,18] of the blend. Before being discharged, the blend was allowed to cool within the mixing chamber (without rotor activity) to 200°C in order to minimize oxidative degradation. For comparison purposes, parallel blank runs on pure components were also made.

Scanning electron microscopy

The melt-mixed blends were manually fractured at liquid-nitrogen temperature. The fracture surface was then sputter-coated with gold and examined using a JEOL JSM-35CF scanning electron microscope at an accelerating voltage of 25 kV.

RESULTS

Mixing torque

Figure 1 gives the variations of mixing torque with blend composition for both blend pairs. For the PPSL/PE blends, the mixing torque deviates negatively from a linear additivity rule:

$$\tau = \phi_1\tau_1 + \phi_2\tau_2 \qquad (2)$$

The maximum deviation lies in the vicinity of $\phi_{PE} \simeq 0.55$. For the PPSH/PE blends, the mixing torque deviates negatively from linear additivity at lower PE levels but positively at higher PE contents.

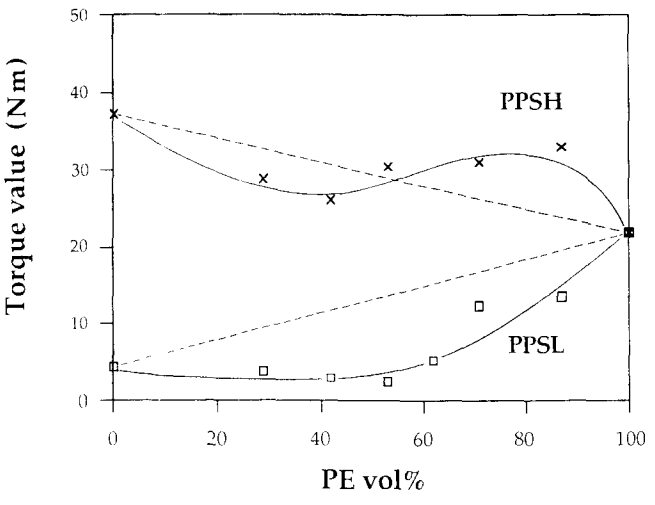

Figure 1 Mixing torque values at 300°C under a fixed rotor rate of 40 rpm

Phase inversion

Shown in *Figure 2* are secondary electron images of surfaces of cryogenically fractured PPSH/PE blends. At a low PE level (*Figure 2a*), PE is the dispersed phase; at higher PE contents (*Figures 2d* to *2f*), PPSH is the dispersed phase. At $\phi_{PE} = 0.42$, two types of morphology were identified. Areas of intermingled and co-continuous phase zones containing droplets of the other phase (cf. *Figure 2b*) may be observed. The phase zones are typically 10–30 μm in transverse dimension. In other regions, the blend exhibits a continuous PPS matrix and large (ca. 10–20 μm in size) PE domains; within each phase zone, micrometre-sized droplets of the other phase are clearly discernible (cf. *Figure 2c* and lower-left part of *Figure 2b*).

For the present purposes, equation (1) can be rewritten as:

$$\phi_1/\phi_2 = \tau_1/\tau_2 \qquad (3)$$

where τ represents the stable torque value of each component phase. The torque ratio of this blend pair is $\tau_{PPSH}/\tau_{PE} = 1.7$, from which equation (3) suggests that phase inversion should occur in the vicinity of $\phi_{PE} = 0.37$, somewhat lower than the experimental observation above.

Figure 3 shows micrographs of cryogenically fractured PPSL/PE blends. At lower PE levels (*Figures 3a* and *3b*), PE is the dispersed phase; at high PE contents (*Figures 3c* to *3e*), PPSL is the dispersed phase. The phase inversion process appears to occur sharply between $\phi_{PE} = 0.53$ and 0.62, from which we may state that phase inversion occurs in the vicinity of $\phi_{PE} \simeq 0.58$. Since the torque ratio of this blend pair is $\tau_{PE}/\tau_{PPSL} = 5$, the corresponding prediction of Sperling's model (i.e. equation (3)) is $\phi_{PE} = 0.83$, in clear disagreement with the experimental observation.

Particle size

Values of the number-average particle diameter in the present blends are compared in *Table 1*. Several preliminary observations may be made. The particle size of the PPSL blends is generally much higher than that of the PPSH blends, attributable to the stronger viscosity mismatch in the former ($\tau_{PE}/\tau_{PPSL} = 5$, whereas $\tau_{PPSH}\tau_{PE} = 1.7$). However, there exists an exception at $\phi_{PE} = 0.87$, where the size of PPSL particles is smaller than that of PPSH particles. In addition, the particle size of PPSL blends increases strongly with increasing volume fraction of the dispersed phase; however, this effect is not apparent in PPSH blends.

Interface morphology

Phase assignments given in the preceding paragraphs were in fact facilitated by the observations that surface features of dispersed PE and PPS particles were characteristically different. *Figure 4a* is a magnified view of the dispersed PE particle surface, where protruding fibrils are clearly seen. *Figure 4b* shows the exposed PPS surface after debonding of PE particles, where pores, resulting from detachment of PE fibrils, are observed. As far as is known, this peculiar interface morphology has never been reported before. Interestingly, the interface morphology is quite different when PPS is the dispersed phase. Given in *Figure 5* is a magnified view of exposed PPS particles, which exhibit an orange-peel appearance.

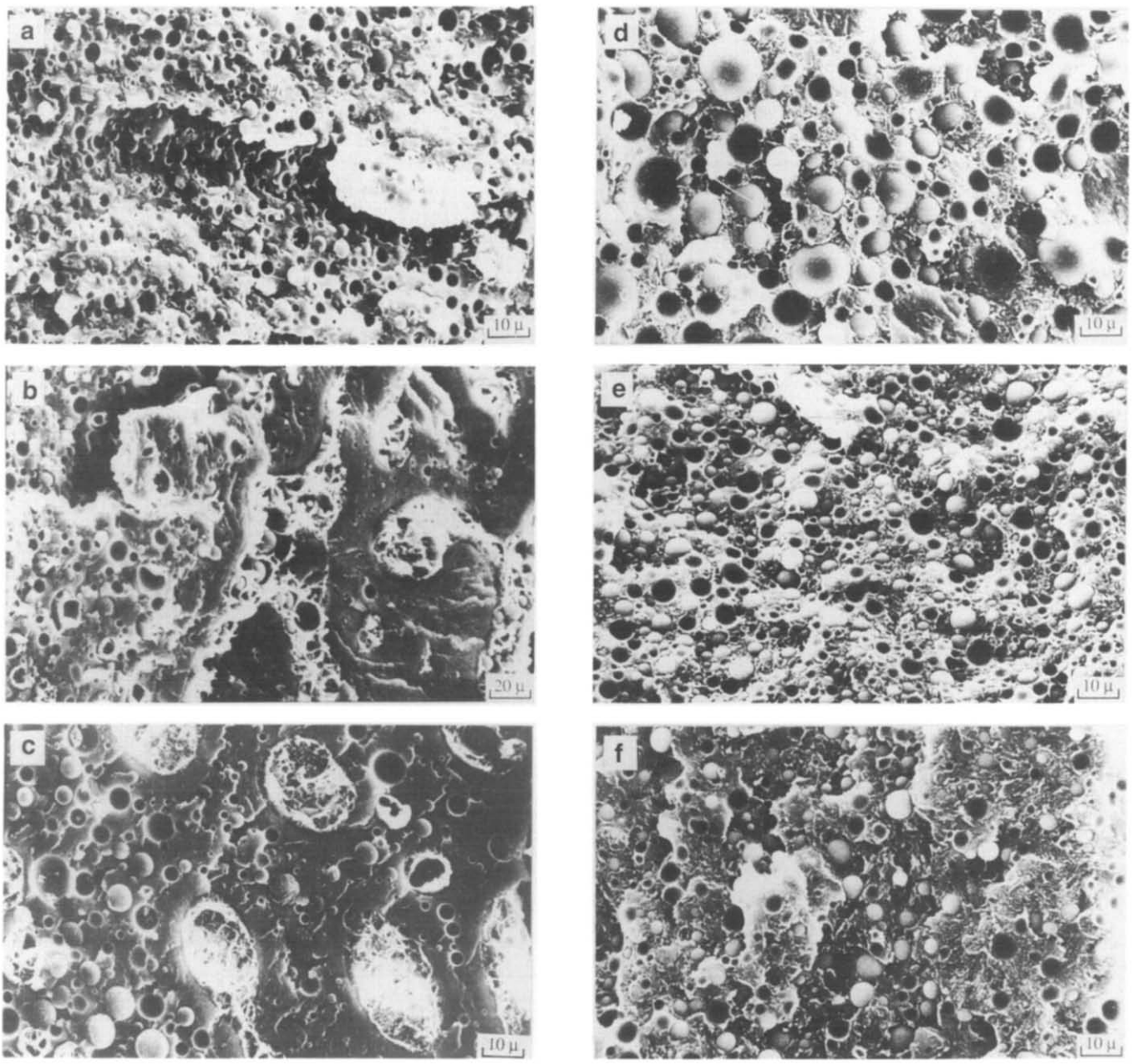

Figure 2 Secondary electron images of surfaces of cryogenically fractured PPSH/PE blends: (a) $\phi_{PE}=0.29$; (b), (c) $\phi_{PE}=0.42$; (d) $\phi_{PE}=0.53$; (e) $\phi_{PE}=0.71$; (f) $\phi_{PE}=0.87$

DISCUSSION

Domain size

Under the premises of shear mixing, consistent elasticity effects and a constant (and reasonably low) volume fraction of the dispersed phase, Wu[19] indicated that the domain size may follow a semiempirical relationship:

$$We = Cp^{\beta} \tag{4}$$

in which $p=\eta_d/\eta_m$ (where subscripts d and m denote the domain and the matrix phases, respectively) is the viscosity ratio, $We=G\eta_m a/\sigma$ (where G is the shear rate, a the number-average particle diameter and σ the interfacial tension) is the dimensionless Weber group, whereas C and β are empirical fitting parameters. For several blend pairs[18,19], it has been shown that $C=4$ and $\beta=0.84$ (when $p>1$) or -0.84 (when $p<1$).

The behaviour of the present blends, however, does not follow equation (4) in a quantitative manner. For example, at a given ϕ_{PE}, equation (4) suggests that a is proportional to p^{β}/η_m. Therefore, at $\phi_{PE}=0.87$, we should have:

$$a_{PPSL}/a_{PPSH}=(\eta_{PE}/\eta_{PPSH})^{0.84}(\eta_{PE}/\eta_{PPSL})^{0.84}$$
$$=[(\tau_{PE}/\tau_{PPSH})(\tau_{PE}/\tau_{PPSL})]^{0.84}=(5/1.7)^{0.84}=2.5$$

in contrast to the experimental value of $a_{PPSH}/a_{PPSL}=2.5/2.9=0.9$. Similarly, at $\phi_{PE}=0.29$, we would expect that:

$$(a_{PE})_{\text{in PPSL}}/(a_{PE})_{\text{in PPSH}}$$
$$=[(\tau_{PE}/\tau_{PPSH})(\tau_{PE}/\tau_{PPSL})]^{0.84}(\tau_{PPSH}/\tau_{PPSL})=21$$

whereas the experimental result is $(a_{PE})_{\text{in PPSL}}/(a_{PE})_{\text{in PPSH}}=12/2.3=5$.

Compare further the blends of $\phi_{PE}=0.29$ and 0.71 in each series. These correspond to reversed phases but the

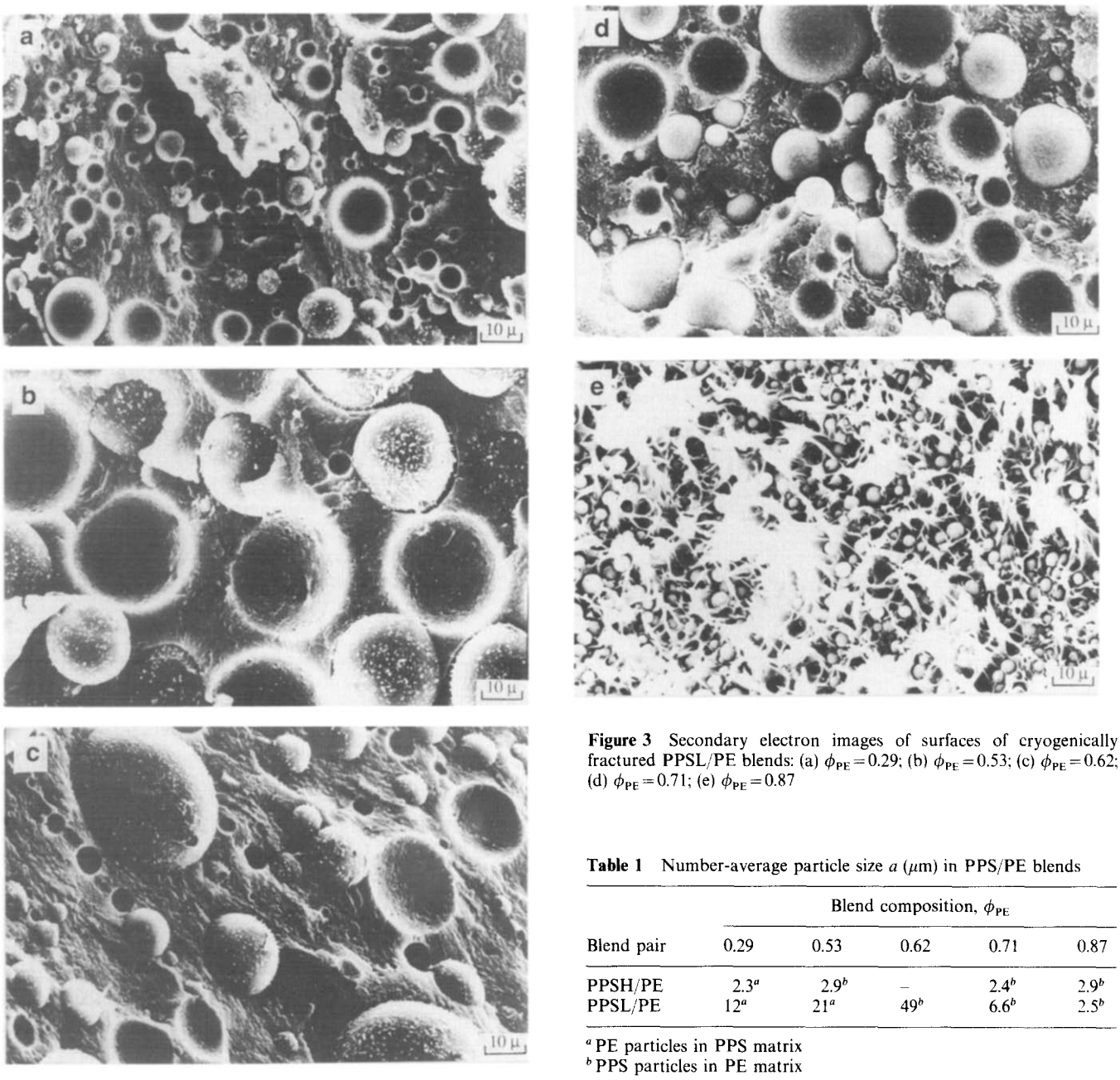

Figure 3 Secondary electron images of surfaces of cryogenically fractured PPSL/PE blends: (a) $\phi_{PE}=0.29$; (b) $\phi_{PE}=0.53$; (c) $\phi_{PE}=0.62$; (d) $\phi_{PE}=0.71$; (e) $\phi_{PE}=0.87$

Table 1 Number-average particle size a (μm) in PPS/PE blends

	Blend composition, ϕ_{PE}				
Blend pair	0.29	0.53	0.62	0.71	0.87
PPSH/PE	2.3[a]	2.9[b]	–	2.4[b]	2.9[b]
PPSL/PE	12[a]	21[a]	49[b]	6.6[b]	2.5[b]

[a] PE particles in PPS matrix
[b] PPS particles in PE matrix

same domain/matrix volume ratios, so that equation (4) should still be applicable. In this case, the predicted ratio of particle diameters is simply $a_{PPSH}/a_{PE}=\tau_{PPSH}/\tau_{PE}=1.7$ for the PPSH blends and $a_{PPSL}/a_{PE}=\tau_{PPSL}/\tau_{PE}=0.2$ for the PPSL blends, as contrasted by the experimental findings of $a_{PPSH}/a_{PE}=2.4/2.3=1.0$ and $a_{PPSL}/a_{PE}=6.6/12=0.55$. We may therefore conclude that the viscosity effects in the present blends are less pronounced than those predicted by equation (4); additional and compensating factors must be present.

One possible origin for the discrepancies above is the elasticity effect. Considering the long-chain branched structure of PPSH and the low molecular weight of PPSL, the relative elasticity of the component polymers is expected to follow the order PPSH > PE > PPSL. It has been demonstrated by van Oene[20] that a droplet of higher elasticity (i.e. higher first normal stress difference, $\sigma_{11}-\sigma_{22}$) tends to increase the effective interfacial tension, and thereby to stabilize the droplet from deformation and breakage; a matrix of higher elasticity bears the opposite effect. The high elasticity of PPSH should therefore enhance dispersion of PE in the PPSH matrix and hinder dispersion of PPSH in the PE matrix. Similarly, the higher elasticity of PE as compared to PPSL should enhance dispersion of PPSL particles in the PE matrix but hinder dispersion of PE particles in the PPSL matrix. This argument, however, can explain only the proximity in size of the PPSH and PPSL particles at $\phi_{PE}=0.87$. For the other discrepancies noted above, the effects of elasticity should be in the same direction as the viscosity effects given by equation (4). It is therefore clear that the elasticity effect is not the major contributing factor to these discrepancies.

As an alternative, we consider the possibility of post-mixing phase coarsening[21]. In view of the relatively long cooling period (approximately 8 min from 300 to 200°C) after the melt mixing process, it is quite likely that significant phase coarsening has occurred. In support of this argument is the observation that the PE phase coalesced (and migrated towards the upper surface)

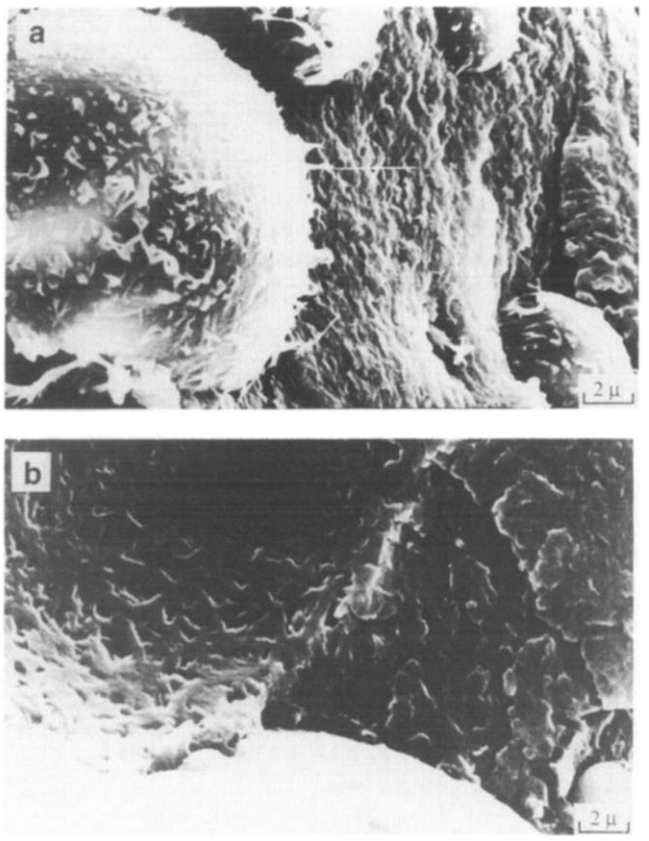

Figure 4 Secondary electron images of cryogenically fractured PPSL/PE blends: (a) protruding fibrils on the surface of a PE particle ($\phi_{PE}=0.29$); (b) pores on the exposed PPS surface after debonding of a PE particle ($\phi_{PE}=0.53$)

Figure 5 Secondary electron image of a cryogenically fractured PPSH/PE blend ($\phi_{PE}=0.53$), showing the orange-peel appearance of PPS particle surface

during the subsequent compression moulding of PPSL blends at 300°C; this phenomenon, however, was less apparent in the case of PPSH blends. The driving force for the coarsening is undoubtedly the high interfacial tension (estimated[17,22] to be ca. 4 mJ m^{-2} at 300°C) as well as the significant density difference between the two phases. To allow for phase coarsening, the dispersed domains must be brought into contact (say, by buoyancy force) first; therefore, a high matrix viscosity should tend to hinder the process. In addition, once the droplets are in contact, the coalescence process (driven by the interfacial tension) is resisted by the *average* viscosity[23] of the two phases. It is therefore clear that a lowering of phase viscosities (especially that of the continuous phase) tends to enhance post-mixing coarsening, in agreement with the observed coarsening phenomenon during compression. In addition, an increase in volume fraction of the dispersed phase may also encourage droplet coalescence owing to decreased distance between particles.

If significant phase coarsening has occurred, the effects should be more pronounced for PPSL blends, especially when PPSL is the continuous phase. This is indeed reflected in the relatively high domain size of PPSL blends and its decreasing tendency near the high ϕ_{PE} end. The pronounced increase of domain size with increasing volume fraction of the dispersed phase in the PPSL series is also consistent with the coalescence effects. In view of the low value of a_{PPSL}/a_{PPSH} at $\phi_{PE}=0.29$ as compared to that predicted by equation (4) (i.e. 5 vs. 21, cf. 'Results'), post-mixing coarsening must also have occurred (although presumably to a less pronounced extent) in PPSH blends. It may therefore be concluded that final morphological features of the present blends reflect significant contributions from not only the dispersion action during melt mixing but also the phase coarsening after cessation of flow.

Phase inversion

In a previous report[13], morphological features of polystyrene/poly(styrene-*co*-butadiene) (PS/SBR) and polypropylene/poly(ethylene-*co*-propylene) (PP/EPR) blends prepared by melt mixing in a Brabender-type internal mixer were studied. Phase inversion was observed to progress gradually with the variation of blend composition, covering typically a composition range of ca. 20 vol%. The transverse dimension of the co-continuous phases was fairly thin, approximately several micrometres. The central composition of the phase inversion process did not follow exactly Sperling's model (i.e. equation (3)), which overestimated the volume fraction of the high-viscosity copolymer phase. Instead, the experimental results were better represented by an empirical equation:

$$\phi_1/\phi_2 = 1.2(\tau_1/\tau_2)^{0.3} \quad (5)$$

where subscripts 1 and 2 denote respectively the high- and the low-viscosity phases. It is noted that equation (5) is asymmetric with respect to the exchange of subscripts, indicating that additional factors may have contributed in an asymmetric manner.

Similar to previous observations, the volume fraction of the high-viscosity phase at phase inversion in the present blends also tends to be overestimated by equation (3) but more closely described by equation (5). The estimated ϕ_{PE} values at phase inversion are 0.41 and 0.57 for the PPSH and the PPSL series, respectively, in excellent agreement with the experimental findings of ca. 0.42 and ca. 0.58. Quintens *et al.*[24] have shown that post-mixing coarsening can result in changes from dual-phase continuity to a typical domain-in-matrix morphology or vice versa, depending on the blend composition. Therefore, the better agreement between equation (5), an asymmetric (and hence theoretically inconsistent) expression, and our experimental observations very likely originates from the significant post-mixing coarsening effects in these blends. As discussed earlier, the extent of post-mixing coarsening depends more

heavily on the matrix viscosity and therefore may contribute more significantly at compositions rich in the low-viscosity phase, i.e. contribute asymmetrically to the blend morphology.

In drastic contrast to the previously studied[13] PS/SBR and PP/EPR blends, however, the phase inversion process in the PPSL blends is rather sharp, without clear evidence of dual-phase continuity. In the case of the PPSH series, co-continuous phases can be identified only in a region-wise manner, with rather coarse phase dimensions (ca. 10–30 μm). These may probably be related to the high interfacial tension (ca. 4 mJ m^{-2}, significantly higher than the estimated[17,22] values of 0.3 mJ m^{-2} for PS/SBR blends and 0.1 mJ m^{-2} for PP/EPR blends at the respective processing temperatures), which resists elongation of phase zones and encourages post-mixing coalescence, the latter being further enhanced by the presence of the low-viscosity PPSL.

Interface morphology

During cooling from the melt state at a moderate rate (i.e. 5–10°C min^{-1}), the crystallization of PPS occurs in the vicinity of 230°C whereas the crystallization of PE occurs near 110°C[25,26]. The orange-peel appearance of PPS particles dispersed in the PE matrix may be simply attributed to the shrinkage of PPS during crystallization at elevated temperatures where the PE matrix remains in the liquid state.

As for the case of PE particles dispersed in the PPS matrix, the situation is more complicated. Simultaneous observations of the protruding fibrils on the surface of PE particles and the corresponding pores at the surface of PPS after detachment of PE particles clearly indicate that this peculiar feature is real, not an artefact of the fracture process. During cooling from the melt state, the PPS matrix solidifies first. The shrinkage of PPS and the incompressible nature of PE melt result in a triaxial compressive stress (i.e. pressure) in the PE droplet and tensile stresses in PPS. These stresses can be rather significant, as the following order-of-magnitude estimates at the idealized elastic limit may show. Consider a PE droplet within a PPS/PE composite matrix of $\phi_{PE} = 0.3$. A 10% increase in crystallinity in PPS during a certain period of PPS solidification may result in an average volumetric shrinkage of ca. 1% for the composite matrix. The volumetric strain in the PE droplet can be in excess of 0.5%, which would translate into a pressure of ca. 10 MPa or 100 bar, since the bulk modulus of PE melt is ca. 2 GPa[17]. This surely represents an overestimation; realistically, mechanisms such as viscoplastic flow of the matrix should be able partly to relax the stresses. The point here is that a significant pressure may indeed develop within PE droplets during the solidification of PPS matrix.

It has been indicated by Cebe and Chung[27,28] that, during crystallization of PPS, a loosely packed structure of thick lamellae is developed first, followed by the formation of thinner lamellae in the interstitial regions of the primary spherulitic structure. It is therefore likely that, during an intermediate stage of PPS solidification where the main structure of thick lamellae has been formed (so that the main body of the PPS matrix is rigid and significant shrinkage stresses have developed) but the interstitial regions are still somewhat fluid, the pressure within PE droplets may force the PE melt into the PPS matrix through the interstitial channels within the PPS spherulites. This explains both the fibril-like appearance as well as the rather uniform distribution of the protrusions on the PE surface.

CONCLUSION

In summary, we have demonstrated that morphological features including the domain size and the apparent phase inversion process of the present PPS/PE blends exhibit significant effects from both the dispersion action during melt mixing and the post-mixing coarsening after cessation of flow. The latter appeared to be the origin of the asymmetric nature of an empirical relationship between the viscosity ratio and the midpoint composition of phase inversion. In addition, interesting morphological features of the PPS/PE interface (i.e. the protruding fibrils on the surface of PE particles and the orange-peel appearance of the PPS particle surface) were explained in terms of the sequential crystallization of PPS and PE.

ACKNOWLEDGEMENTS

Thanks are due to Mr Min-Jih Kuo of USI Chemical, who kindly provided molecular-weight information for the PE sample. Support from the National Cheng-Kung University and the ROC Ministry of Education endowed to T.H.C. in the form of leave-with-pay is gratefully acknowledged. This work is financed in part by the ROC National Science Council under Contract Number NSC-82-0405-E110-033.

REFERENCES

1 Newman, S. in 'Polymer Blends' (Eds. D. R. Paul and S. Newman), Academic Press, New York, 1978, Ch. 13
2 Bucknall, C. B. in 'Polymer Blends' (Eds D. R. Paul and S. Newman), Academic Press, New York, 1978, Ch. 14
3 Maxwell, B. and Jasso, G. I. *Polym. Eng. Sci.* 1983, **23**, 614
4 Paul, D. R. in 'Polymer Blends' (Eds D. R. Paul and S. Newman), Academic Press, New York, 1978, Ch. 1
5 Kresge, E. N. in 'Polymer Blends' (Eds D. R. Paul and S. Newman), Academic Press, New York, 1978, Ch. 20
6 Han, C. C. 'Multiphase Flow in Polymer Processing', Academic Press, New York, 1981
7 Manas-Zloczower, I., Nir, A. and Tadmor, Z. *Rubber Chem. Technol.* 1984, **57**, 583
8 Utracki, L. A. and Shi, Z. H. *Polym. Eng. Sci.* 1992, **32**, 1824
9 Avgeropoulos, G. N., Weissert, F. C., Biddison, P. H. and Bohn, C. G. A. *Rubber Chem. Technol.* 1976, **49**, 93
10 Jordhamo, G. M., Manson, J. A. and Sperling, L. H. *Polym. Eng. Sci.* 1986, **26**, 517
11 Miles, I. S. and Zurek, A. *Polym. Eng. Sci.* 1988, **28**, 796
12 Favis, B. D. and Chalifoux, C. P. *Polymer* 1988, **29**, 1761
13 Ho, R. M., Wu, C. H. and Su, A. C. *Polym. Eng. Sci.* 1990, **30**, 518
14 Paul, D. R. and Barlow, J. W. *J. Macromol. Sci. (C)* 1980, **18**, 109
15 Sperling, L. H. 'Interpenetrating Polymer Networks and Related Materials', Plenum, New York, 1981
16 Stacy, C. J. *J. Appl. Polym. Sci.* 1986, **32**, 3959
17 van Krevelen, D. W. 'Properties of Polymers', Elsevier, Amsterdam, 1976
18 Serpe, G., Jarrin, J. and Dawans, F. *Polym. Eng. Sci.* 1990, **30**, 553
19 Wu, S. *Polym. Eng. Sci.* 1987, **27**, 335
20 van Oene, H. *J. Colloid Interface Sci.* 1972, **40**, 440
21 Quintens, D., Groeninckx, G., Guest, M. and Aerts, L. *Polym. Eng. Sci.* 1990, **30**, 1484
22 'Polymer Handbook' (Eds. J. Brandrup and E. H. Immergut), Wiley, New York, 1989
23 Carriere, C., Cohen, A. and Arends, C. B. *J. Rheol.* 1989, **33**, 681
24 Quintens, D., Groeninckx, G., Guest, M. and Aerts, L. *Polym. Eng. Sci.* 1990, **30**, 1474
25 Nadkarni, V. M. and Jog, J. P. *J. Appl. Polym. Sci.* 1986, **32**, 5817
26 Chen, T. H. and Su, A. C. in preparation
27 Cebe, P. and Chung, S. *Polym. Compos.* 1990, **11**, 265
28 Chung, J. S. and Cebe, P. *Polymer* 1992, **33**, 2312